Decision Letter (TDE-2018-0037.R3)

From: r.finnie@future-science.com

To: josemariabermudez@gmail.com

CC: analiasimonazzi@gmail.com, aliciagracielacid@gmail.com, alejandrojparedes@gmail.com, lschofs@vet.unicen.edu.ar, gonzo@unsa.edu.ar, sdpalma@fcq.unc.edu.ar

Subject: Therapeutic Delivery - Decision on Manuscript ID TDE-2018-0037.R3

Body: 26-Jul-2018

Dear Dr. Bermúdez,

It is a pleasure to accept your manuscript entitled "Development and in vitro evaluation of solid dispersions as strategy to improve albendazole biopharmaceutical behavior" in its current form for publication in Therapeutic Delivery. Our production department will be in touch with the galley proofs - please do let me know if you are going to be away at any point and unable to check them.

Please note, we are able to offer a fast-track production service, for a fee of $800, providing guaranteed online publication within 3 weeks (subject to turnaround of proofs by the author within 3 working days). Should you be interested in this service, please let me know.

Common errors to check and watch out for when approving your proofs (those that are harder for our copy editors to catch):
– Have you listed all your co-authors, and spelt their names correctly?
– Have you included correct affiliation details for yourself and your co-authors?
– Have you included all your funding information, including grant numbers, in the acknowledgement section (i.e., NIH, Wellcome Trust, etc.)?

Although corrections can be made after publication, these will only be carried out if they are deemed by the editor to be critical to the understanding of the article. So it is important to check information such as the above is correct when the article goes to print, as it cannot always be corrected at a later date.

Please note that the version uploaded to the ScholarOne system is classified as the 'Author's final version'. You are able to upload this version to your institutional repository if required. If you would like us to send you a copy of the author's final version, please let me know. For all other uses of this article version, please refer to the journal's self-archive policy.

Therapeutic Delivery offers an open access option, whereby for a fee, articles can be made freely available for all to read. As of 2016, the journal saw over 10-times more readers for articles that were freely available, showing a distinct advantage for the open access option. Pricing varies by article type; for peer-reviewed content (i.e., Original Research or Review articles), the fee is $2,500; for content not reviewed externally (i.e., Editorials or Commentaries), the fee is $850. For more information, visit our website here: https://www.future-science-group.com/services/for-researchers/open-access/. If you are interested in taking this option, please let me know.

In addition, Colour Printing can enhance the impact of your article's figures with readers. Should you wish your figures to appear in colour in the print issue of the journal, there is a fee of $220 for the first figure and $135 for each subsequent figure. Please note that charges for colour figures only apply for print issues of the journal; all figures appear online in colour at no cost. If you are interested in having one or more of your figures printed in colour, please let me know.

Finally, if your institution does not already subscribe to Therapeutic Delivery, it would be great if you would be willing to email your librarian to recommend the journal to them (or alternatively, reply to this email if this is of interest, and we can contact your librarian to discuss free trial and subscription options).

Thank you for your contribution. On behalf of the Editors of Therapeutic Delivery, we look forward to working with you in the future.

Sincerely,
Rhiannon Finnie
Commissioning Editor, Therapeutic Delivery
r.finnie@future-science.com

Date Sent: 26-Jul-2018

Development and in vitro evaluation of solid dispersions as strategy to improve albendazole biopharmaceutical behavior

Journal:	*Therapeutic Delivery*
Manuscript ID	TDE-2018-0037.R3
Manuscript Type:	Preliminary Communication
Keywords:	Solid dispersions, Poloxamer, Albendazole

Abstract

Aim: Solid dispersions using Poloxamer 407 as carrier were developed to improve albendazole solubility and dissolution profiles. **Methodology:** Albendazole/Poloxamer solid dispersions were prepared, and dissolution profiles were mathematically modeled and compared with physical mixtures, pharmaceutical albendazole, and a commercial formulation. **Results:** Poloxamer 407 increased exponentially albendazole solubility, in about 400% when 95% w/w of polymer compared with its absence. Solid dispersions initial dissolution rate was 3 to 20-fold higher than physical mixtures, the drug and the commercial formulation. All the solid dispersions required less than 2.2 min to reach an 80% of albendazole dissolution, while the commercial formulation needed around 40 min. **Conclusion:** Solid dispersions improved albendazole solubility and dissolution rate, what could result in a faster absorption and an increased bioavailability.

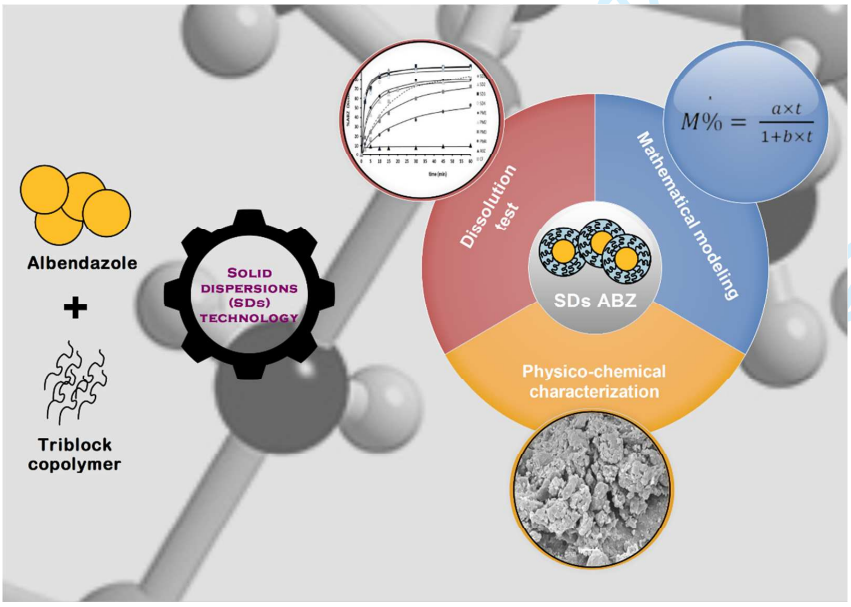

Keywords: Solid dispersions; Poloxamer; Albendazole; Solubility; Initial dissolution rate; Dissolution efficiency; Lumped model.

Introduction

It has been well proven that solubility and gastrointestinal permeability play a crucial role in controlling rate and extent of drug absorption, and therefore, *in vitro* drug product dissolution can be correlated with *in vivo* bioavailability [1]. A fundamental property for drug absorption after oral administration is its aqueous solubility. Evidence suggests that a drug molecule must be enough soluble in water to be easily administered to the cell membrane, but it must be also enough hydrophobic to pass through it [2].

For this reason, while a drug with poor aqueous solubility will exhibit a limited dissolution rate, a drug with poor membrane permeability will exhibit a limited permeation rate. This has been one of the most critical issues in pharmaceutical research field for many decades.

Literature has emphasized the increased number of insoluble drugs that are candidates to be formulated in a dosage form [3, 4]. Consequently, pharmaceutical research area that focus on enhancing the oral bioavailability of active agents aims to improve the solubility of poorly water soluble drugs, to enhance their dissolution rate and absorption kinetics. Moreover, these drugs offer limited administration routes due to their few formulation alternatives [5].

Albendazole (ABZ) is widely used in both veterinary and human medicine for the treatment of parasitic infections causing intestinal disorders [6, 7]. ABZ has low aqueous solubility and high permeability, and therefore, it is not well absorbed in the gastrointestinal tract. As a consequence, it is classified as a Class II drug by the Biopharmaceutics Classification System [1], having a low dissolution rate [8, 9].

Currently ABZ is available as tablets or suspensions with high doses of active agent and its therapeutic efficacy is compromised due to its low aqueous solubility [10]. To overcome these drawbacks, it is important to increase the aqueous solubility and therefore the

dissolution rate of ABZ. In this context, the challenge for this broad-spectrum drug lies in the development of new formulations. Following this guideline, different strategies have been developed to improve ABZ bioavailability, such as formulation of solid dispersions [11-14], complexation with cyclodextrin [15, 16], co-grinding [5], the synthesis of new analogs with higher solubility [17, 18], microcrystals [19], nanocrystals [20], and more recently, several nano-particulate formulations [21-24]. However, the need of reproducible, inexpensive, scalable and organic solvent-free approaches to carry ABZ still remains a challenge.

Solid dispersions (SDs) are considered one of the most successful strategies to improve the dissolution profile of poorly soluble drugs. In 1971, Chiou and Riegelman defined SDs as dispersions of one or more active ingredients in inert carriers or matrixes at solid state prepared by melting (fusion), solvent, or melting-solvent procedures [25]. SDs can be classified into four generations according to the physical state of the carrier [26, 27]. First generation SDs are crystalline and consist of a crystalline drug dispersed in a crystalline carrier forming an eutectic or monotectic mixture [28-31]. The second generation of SDs includes amorphous carriers which are mostly polymers, such as crospovidone [32] and hydroxypropylmethylcellulose [33], among others. In the third generation of SDs, surface active agents or self-emulsifier are incorporated as carriers or additives and help to improve problems such as precipitation. The addition of surfactants and emulsifiers in SDs improves not only the dissolution profile, but also the physical and chemical drug stability. Finally, the fourth generation of SDs consists of a controlled release solid dispersion containing poorly water-soluble drugs with a short biological half-life [34].

In SDs the polymer serves as a carrier in which the drug is dispersed. Therefore, polymer selection is very important since it influences manufacturing, bioavailability, and stability of the SDs. Initial assessment of potentially “useful” excipients should be based on basic

physicochemical properties of the polymers, such as glass transition temperature (Tg), hygroscopicity, and solubilization capacity, among others. Several carriers were evaluated for ABZ SDs, such as polyvinylpyrrolidone [11, 35], polyethylene glycol [14, 36], Gelucire [36], and Poloxamer 188 [12].

Poloxamers, a family of triblock copolymers of ethylene oxide and propylene oxide, are nonionic surfactants with solubilizing properties. They are marketed under a variety of trade names, such as Pluronic™ from BASF. Poloxamers are available in different ethoxylated content and molecular weight. Their polymeric nature makes them suitable for most of the standard procedures used to prepare SDs. Moreover, they present an improved miscibility with many pharmaceutical actives due to their structure in comparison with nonpolymeric surfactants. In particular, Poloxamer 407 (P 407) is accepted by FDA as an "inactive" ingredient for different types of preparations (e.g., IV, inhalation, oral solution, suspension, ophthalmic or topical formulations) [37].

The aim of this work was to prepare, characterize and *in vitro* evaluate ABZ SDs, prepared by the fusion method, based on P 407 for enhancing the solubility and dissolution rate of the drug, pursuing the improvement of its absorption rate, and then its bioavailability. In this context, solubility studies and dissolution test were performed to compare the SDs behavior with other ABZ formulations. The obtained data were fitted using a mathematical model developed and validated by our research group, which allowed to calculate several parameters of pharmaceutical relevance. An analysis based on the independent method was also performed to compare the dissolution profile of SDs with different ABZ/P 407 proportions.

Materials and methods

Materials

ABZ of pharmaceutical grade was purchased from Todo Droga (Córdoba, Argentina) and Poloxamer 407 from BASF® (Germany).

The commercial formulation of ABZ (CF) was Vermizole® (Lafedar Laboratory, Argentina). Each tablets contains 200 mg of ABZ and the following excipients: magnesium stearate (2 mg), sodium lauryl sulfate (8 mg), croscarmellose sodium (32 mg), lactose SD (enough quantity for 400 mg), sodium glycolate starch (18 mg), pregelatinized starch (51 mg), and hydroxypropylmethylcellulose (4 mg) [101]. Apparently, according to the reported excipients used in the preparation of the tablet, this formulation is prepared by direct compression.

ABZ does not present enantiomers, although albendazole sulphoxide, its active metabolite does due to the presence of a chiral sulfur atom [6, 38].

ABZ ~~T~~tablets ~~containing 200 mg of the drug per unit~~ were pulverized and sieved. The 210-µm size fraction was used for dissolution tests. The powder was stored in a screw-cap vial until use.

All other reagents were of analytical grade.

SDs preparation.

Four SDs using P 407 as carrier with 5, 10, 25 and 50 % w/w of ABZ (SD1, SD2, SD3 and SD4, respectively) were prepared by the fusion method. Briefly, the drug was homogeneously dispersed by stirring in the molten carrier at 63 °C. The resulting homogeneous preparation was rapidly cooled in liquid nitrogen and then pulverized. The 210-µm particle size fraction was obtained by sieving and kept in a screw-capped glass vial until use. Physical mixtures (PMs) were prepared by mixing the components in the same

Formatted: Superscript

proportions in a Laboratory-scale V-blender for 5 min (5, 10, 25 and 50 % w/w of ABZ, named PM1, PM2, PM3 and PM4, respectively), using the 210-µm particle size fractions of sieved ABZ and P 407. The powders were stored in a screw-cap vial until use.

Physico-chemical characterization of the materials.

X-ray diffraction (XRD) and Fourier Transform Infrared (FTIR) spectroscopy.

Pharmaceutical grade ABZ, P 407, SD4, and PM4 were analyzed by X-ray diffraction using a DRX Philips PW1800 diffractomer. Assays were performed at 40 KV and 30 mA in a range of 5-70 ° 2Theta at a rate of 0.02 ° 2Theta / s.

These samples were also characterized by FTIR spectroscopy using a Spectrum GX-Perkin Elmer Spectrometer over the region 4000-400 cm^{-1}, after mixing them with potassium bromide (spectroscopic grade) and compressing into disks using a hydraulic press.

Scanning Electron Microscopy (SEM)

The morphology of pharmaceutical grade ABZ, P 407, SD3, SD4, PM3, and PM4 was evaluated by SEM. Samples were gold covered (Denton Vacuum metallizer, LLC, Desk-IV) and observed by a Scanning electron microscope (JEOL JSM-6480LV, Japan).

Differential Scanning Calorimetry (DSC)

Pharmaceutical grade ABZ, P 407, SD4, and PM4 DSC thermograms were obtained using a Q200 (TA instrument). Samples were accurately weighed into hermetic aluminum pans, then hermetically sealed with aluminum lids and heated from 25°C to 250°C at a heating rate of 10°C/min under constant purging of dry nitrogen 20 ml/min. An empty hermetic aluminum pan, sealed in the same way as the sample, was used as reference.

Phase solubility studies

An excess of ABZ was added to 5 ml of a 0.1 N HCl containing increasing concentrations of P 407 (1, 3, 5, 10 and 15 % w/v) in sealed glass vials. Then they were placed in a bath under stirring at room temperature for 96 hours to reach solubility equilibrium. After that, suspensions were filtered through a 0.45 µm mixed cellulose ester membrane, and the filtrate was assayed for ABZ concentration spectrophotometrically at λ=302 nm, using the corresponding calibration curve constructed with standard solutions of ABZ in 0.1 N HCl.

Saturation solubility studies

For saturation solubility studies, an excess amount of pharmaceutical grade ABZ, SDs and PMs was added into sealed glass vials with 10 ml of 0.1 N HCl. They were maintained in a water bath under stirring at 37 °C for 4 days. After that, the samples were filtered through a 0.45 µm mixed cellulose ester membrane, and the filtrate was analyzed spectrophotometrically to determine ABZ concentration.

Biopharmaceutical characterization

Dissolution tests of SDs, PMs, pharmaceutical grade ABZ and CF were performed using an USPXXIV dissolution apparatus 2 (SOTAX AT 7 smart) at 37±0.5°C and under stirring at 50 rpm. The necessary amount of powdered samples having 50 mg of ABZ was weighed accurately and added into 900 ml of filtered and degassed 0.1 N HCl used as dissolution medium. At predetermined intervals of time four-milliliter of filtered aliquots were withdrawn and replaced by fresh medium to keep the volume constant. The concentration of dissolved drug was determined spectrophotometrycally.

Dissolution data were analyzed by a lumped second-order kinetic model developed [39] and validated [40] by our research group. To compare the different dissolution profiles, initial dissolution rate (*IDR*), sampling time (t_{tmin}), dissolution time ($t_{X\%}$), dissolution efficiency (*DE*), similarity and difference factors (f_1 and f_2, respectively) and mean dissolution time (*MDT*) were calculated, according to the independent statistical analysis methods [41].

Data analysis

Solubility and dissolution assays were performed by triplicate and data are presented as the mean ± the standard deviation (s). Statistical analysis was performed using Polymath 6.0 software. For statistical comparisons, a p-value less than 0.05 ($p < 0.05$) was considered significant.

Results and discussion

Physico-chemical characterization of the materials

X-ray diffraction and IR spectroscopy

SD4 and PM4 were selected to perform characterization studies because ABZ was in major proportion in them and so, any change or interaction would be easier detected.

Samples of pharmaceutical grade ABZ, P 407, SD4 and PM4 were analyzed by XRD in order to evaluate their crystalline state. As shown in Fig. 1, the diffraction profile of ABZ evidenced its crystalline nature, showing numerous diffraction peaks at 6.80°, 11.30°, 13.8°, 17.9°, 19.5°, 20.8°, 22.1°, 24.43°, 24.6°, 27.2°, 28.4° and 29.9°, in concordance with the reported by other authors [13, 42]. In XRD diffractogram, the characteristic peaks of P 407 were observed at 19.2° and 23.2°, as reported in literature [43]. (Fig. 1).

In both PM4 and SD4, the XRD patterns showed no changes in the signals assigned to

the drug and the polymer, indicating no interactions. However, it was observed that some of the characteristic peaks of ABZ were reduced or even absent in SD4, which could be suggesting a slightly reduction in crystallinity when compared to PM4. This could lead to an improvement in solubility because amorphous forms are more easily solubilized than the crystalline forms.

FTIR spectra of ABZ, P 407, PM4 and SD4 (Fig. 2) were compared to evaluate possible interactions between the drug and the polymer or changes in the wavelength of the functional groups of the drug.

ABZ is a N-aryl secondary urethane, that exhibits a medium intensity peak at 3322 cm^{-1} attributed to N-H stretching [44]. The band due to the carbonyl stretching vibration, termed as amide I band of urethanes, occurs in the region of 1740-1680 cm^{-1}. In view of these, the band present at 1711 cm^{-1} was assigned to the amide I vibration of the carbamate group [44]. Urethanes also exhibit amide III band just like amides, but in the region of 1260-1220 cm^{-1}. In this line, the very strong band present at 1271 cm^{-1} was due to the combination of N-H deformation and C-N stretching vibration motion. In the ABZ FTIR spectrum the signals corresponding to aromatic ring stretching occurred at 1630 cm^{-1}. The P 407 FTIR spectrum showed the principal absorption bands at 1343 cm^{-1} and 1110 cm^{-1} corresponding to in-plane O-H bend and C-O stretching, respectively, coinciding with the reported for P 407 [45]. All signals recently explained remained practically unaltered for SD4 and PM4 at the same wave numbers. In both preparations, the peaks corresponding to each component were observed and no new peaks appeared. For this reason, it could be concluded that there were no chemical interactions among ABZ and P 407 as consequence of their close contact in both the SD and PM or during their manufacturing process.

Scanning Electron Microscopy (SEM)

Pharmaceutical grade ABZ, P 407, SD3, SD4, PM3 and PM4 were characterized by SEM in order to determine the morphology of the drug within the polymeric matrix. SEM images presented ABZ as small particles of irregular shape and rough surface (Fig. 3a). P 407 was observed as large spheres of smooth surface and irregular shape of different sizes (Fig. 3b). Figures 3c and 3d showed that SD3 and SD4 presented rough surface particles of different sizes, where the spherical particles of P 407 and irregular particles of ABZ could not be distinguished. In Figures 3e and 3f, corresponding to PM3 and PM4, respectively, ABZ was distributed on the surface of P 407 maintaining its structure.

Differential Scanning Calorimetry

DSC analysis of pharmaceutical grade ABZ, P 407, SD4 and PM4 (Fig. 4) was carried out to determine the thermal behavior of the samples and the formation of amorphous SDs, which would be indicated by the attenuation or disappearing of the drug melting peak in the thermogram.

ABZ and P 407 presented an endothermic peak at 214.54°C and 53.28°C, respectively, corresponding to their reported melting points [7]. However, an overlap of two peaks was observed in the ABZ run, probably because no recrystallization process of the drug was carried out. This behavior was also reported by other authors [46]. Regarding the binary mixtures, it could be detected that the endothermic peak of the drug was attenuated in the PM, whereas it almost disappeared in the SD, probably because ABZ got dissolved in the molten carrier throughout the test. The peak corresponding to the melting temperature of the carrier did not undergo a major change neither in the PM nor in the SD, revealing an ordered state of P407 in both preparations. However, the SD4 plot showed the peak corresponding to P 407 as

a broad diffuse and displaced endotherm, what would be indicating the formation of a eutectic mixture between the two components (drug and polymer) during the assay.

Phase solubility studies

As previously mentioned, P 407 has surfactant properties with a critical micelle concentration (CMC) of 2.8 µM [47]. Thus, an increase in ABZ solubility caused by this polymer would be expected.

Results indicated that the solubility of ABZ increased linearly (from 0.23 to 0.91 mg/ml) along with the concentrations of the surfactant polymer in the solution from 0% to 15% (w/v), following a linear equation with a slope of 0.042±0.005 and an intercept of 0.32±0.04 (R^2 = 0.945). This result is similar to that reported by Torrado et al. [11].

This could be because at very low concentrations, the P 407 only exists as individual strings, but as the concentration of P 407 increases reaching the CMC, the polymer chains start to associate to form micelles, thus the hydrophobic part of the copolymer avoid contact with the aqueous medium in which it is diluted [48]. These micelles have hydrophobic core of PO chain and hydrophilic shell formed by EO chains. The hydrophobic PO core can incorporate water insoluble molecules, promoting faster and more complete solubility [47].

The increase in the solubility of ABZ could be also explained by the decrease in the interfacial tension between the drug and the medium of the solution provoked by the P 407 [49].

Saturation solubility studies

The saturation solubility of ABZ as a function of P 407 proportion followed a unique curve (standard deviation below 6%), regardless of the type of binary mixture (SD or PM).

The saturation solubility showed an exponential growth when polymer concentration increased. Polymer at 95 %w/w caused an increase in ABZ solubility of about 4-fold with respect to solubility in the absence thereof. However, for Poloxamer proportions lower than 50% in the mixtures, the saturation solubility reached a plateau with a value two times higher than that corresponding to ABZ (0.398 mg/ml).

The data were modeled using Equation 1 with a correlation index of $R^2 = 0.9842$ (Fig. 5).

$$SS = 0.821 + 6.43E - 08 \times \exp(0.168 \times P\%) \qquad \text{(Eq. 1)}$$

Where SS is the ABZ saturation solubility in mg/ml and P% is the Poloxamer percentage in the mixture (%w/w).

Biopharmaceutical characterization

Increasing the dissolution rate of a drug may result in an improvement in its absorption kinetic, leading probably to an enhancement in its bioavailability. This could result in a reduction in the dose needed to reach the therapeutic effect, which is relevant since ABZ is poorly absorbed from the gastrointestinal tract at the usual therapeutic doses, and adverse effects have generally been restricted to gastrointestinal disturbances associated more frequently with high doses. Therefore, grater ABZ solubility and absorption rate would probably help in reducing the therapeutic doses, avoiding adverse effects.

In this context, dissolution profiles of the different SDs in 0.1 N HCl were studied and compared with the PMs, the CF and pharmaceutical grade ABZ (Fig. 6).

The experimental data of the cumulative amount of dissolved ABZ profiles were well correlated by a model previously developed and validated by our research group [39, 40].

This simple model can lump together both diffusional and polymer relaxation steps present in this process, and it is represented by Equation 2 [40]:

$$M\% = \frac{a \times t}{1 + b \times t} \quad \text{(Eq. 2 [40])}$$

Where M% is the percentage of drug dissolved at time t, and parameters *a* and *b* are given in (% min^{-1}) and (min^{-1}), respectively. Table 1 shows the values of the parameters *a* and *b* and the corresponding correlation coefficient for SDs, PMs, ABZ and CF.

Interestingly, the value of the parameter *a* is the *IDR* [40], since the dissolution rate at any time is given by:

$$\frac{dM\%}{dt} = \frac{a}{(1 + b * t)^2} \quad \text{(Eq. 3 [40])}$$

And therefore, when $t = 0$, the *IDR* is:

$$IDR = \left.\frac{dM\%}{dt}\right|_{t=0} = a \quad \text{(Eq. 4)}$$

Significant differences in the *IDR* were observed between SD and CF, ABZ and PM samples (3 to 20-fold). Although the values of the saturation solubility were similar when the same P 407 proportion for both SDs and PMs, the *IDR* were remarkably different. While all the SDs presented values greater than 60 % min^{-1}, neither of the PMs reached 25 % min^{-1}. On the other hand, the CF *IDR* was almost 10-fold lower than the SDs.

The model allowed calculating another interesting parameters of pharmaceutical relevance, which are also shown in Table 1. While t_{Xmin} corresponds to the percentage amount of drug dissolved at a given time, $t_{X\%}$ is the time needed to dissolve a certain percentage amount of drug (Eq. 5). For example, $t_{80\%}$ is the time needed to reach an 80% of dissolved drug, and this value can be used as an acceptance limit according to Pharmacopeias [41],

considering it an immediate drug delivery if lower than 45 min.

$$t_{X\%} = \frac{X\%}{(a - b \times X\%)} \qquad \text{(Eq. 5 [41])}$$

On the other hand, *DE* is defined as the ratio between the area under the profile curve up to a certain final time t_F and the area of the rectangle corresponding to 100% dissolved at the same time [41]. The importance of *DE* lies in considering both the dissolved amount and the dissolution rate. Using our model, *DE* for a final time t_F, is given by:

$$DE = \frac{\int_0^{t_F} M\%\ dt}{100 \times t_F} = \frac{\frac{a}{b^2}[\![b \times t_F - \ln(1 + b \times t_F)]\!]}{100 \times t_F} \qquad \text{(Eq. 6 [41])}$$

Although *IDR* of pharmaceutical grade ABZ was greater than or equal to PM3, PM4 and CF, it has to be also taken into account the percentage amount dissolved at different times (t_{tmin}). When the cumulative amount of ABZ dissolved from this sample reached near 9%, the dissolution almost stopped, at least for the tested 60 minutes. Besides the differences found in the *IDR* between SD and PM samples previously mentioned, significant differences in the t_{30min} (between 20% and 40% approximately) were observed. Regarding to the $t_{80\%}$, all the SDs presented values lower than 2.2 min, meaning that the behavior corresponded to an immediate delivery. Only PM1 reached an 80% of drug dissolution during the evaluated period of time, while the CF $t_{80\%}$ was just under the acceptance limit. The *DE* values were higher for all the SDs than for the corresponding PMs, CF and ABZ of pharmaceutical grade, showing clearly that these products are the best option due to both their high dissolution rate and percentage of ABZ dissolved.

Differences in the dissolution profiles may be explained by the manufacture process of the SD, which impacts in their solid state properties. In the SD, the drug is already present in the molecular state as a "solid solution," and thus the step of drug dissolution is bypassed.

When the drug is part of the SD, its dissolution may be carrier mediated. Initially, a polymer-rich diffusion layer is formed between the solid dispersion and the dissolution medium. After diffusion of ABZ into the polymer-rich phase, the drug is further released into the dissolution medium [50].

To compare the dissolution profiles between the SDs with different ABZ/P 407 proportions, independent statistical analysis methods were chosen. These methods include ratio tests and pair-wise procedures [41]. The pair-wise procedures include the difference and similarity factors (f_1 and f_2, respectively) [51-53]. The first one describes the error between two dissolution curves over all time points, and is defined as:

$$f_1 = \frac{\sum_1^n |R_i - D_i|}{\sum_1^n R_i} \times 100 \qquad \text{(Eq. 7 [51])}$$

Where R_i and D_i are the percent dissolved of the reference and the test sample at each time point i, and n is the number of experimental samples. This percent error is equal to zero when the test and drug reference profiles are identical.

On the other hand, f_2 is defined as the logarithmic transformation of the sum-squared error of differences between the test and the reference product over all time points:

$$f_2 = 50 \times log\left\{\left[1 + \left(\frac{1}{n}\right) \sum_1^n (R_i - D_i)^2\right]^{-0.5} \times 100\right\} \qquad \text{(Eq. 8 [51])}$$

The "Center for Drug Evaluation and Research" (Food and Drug Administration, USA) and the "Human Medicine Evaluation Unit of the European Agency for the Evaluation of Medicinal Products" have established as a criterion to consider similar two dissolution profiles, values of f_1 lower than 15 (0 - 15) and f_2 higher than 50 (50 – 100).

Since no significant differences were observed between the SDs dissolution profiles, all the data were fitted together using a unique curve, which model parameters a and b were 70.4 %

min^{-1} and 0.7 min^{-1}, respectively. To compare the dissolutions profiles between the different SDs, f_1 and f_2 were calculated using the unique curve profile as reference. Values of f_1 and f_2 were 0.9 and 95.0 for SD1, 1.8 and 85.9 for SD2, 1.6 and 87.3 for SD3, and 2.7 and 80.6 for SD4, respectively. These results suggest that the profiles of the different SDs prepared in this work were similar. This is important from a practical point of view when developing a formulation, since a tablet with an adequate amount of drug and an acceptable final weight could be designed.

Independent statistical analysis methods also include ratio tests that are relations between parameters obtained from the release assays of different formulations. Among these parameters, the *MDT* value is one of the most frequently used (Eq. 9), and it was calculated for the SDs to confirm the previously found from the analysis of f_1 and f_2.

$$MDT_{X\%} = \frac{\sum_{j=1}^{n} t_{jm} \times \Delta M\%}{\sum_{j=1}^{n} \Delta M\%} \qquad \text{(Eq. 9 [41])}$$

Where $t_{jm} = (t_j + t_{j-1})/2$ is the midpoint time between two samples and $\Delta M\%$ is the additional amount of drug release between t_j *and* t_{j-1}. However, as we pointed out previously, since our model fitted very well the experimental data, $MDT_{X\%}$ can be calculated as:

$$MDT_{X\%} = \frac{\int_0^{M\%_j} t \times dM\%_j}{\int_0^{M\%_j} dM\%_j} \qquad \text{(Eq. 10)}$$

Considering Equation 3:

$$MDT_{X\%} = \frac{\int_0^{t_{X\%}} \frac{a \times t}{(1+b \times t)^2} dt}{M\%(t_{X\%})} \qquad \text{(Eq. 11)}$$

Finally:

$$MDT_{X\%} = \frac{a}{b^2} \frac{\left[ln(1+b \times t_{X\%}) - \frac{b \times t_{X\%}}{(1+b \times t_{X\%})}\right]}{M\%(t)} \qquad \text{(Eq. 12)}$$

M% ($t_{X\%}$) is the percent of drug accumulated at $t = t_{X\%}$, and the value of t_X is obtained from Equation 5. The values of $MDT_{80\%}$ were 6.7, 6.0, 7.3 and 8.2 min for SD1, SD2, SD3 and SD4, respectively, and 6.9 min for the unique curve that fitted all the data. There were no statically significant differences between them, confirming the similarity in the dissolution profiles of the SDs.

Finally, ABZ initial intrinsic dissolution rate (*IIDR*) was calculated as a function of the ABZ content for the SDs (Eq. 13), and PMs (Eq. 14), and compared with ABZ of pharmaceutical grade (Fig. 7).

$$IIDR_{SD}\ (\frac{\mu g}{ml.min}) = -0.036 \times ABZ\% + 40.38 \qquad \text{(Eq. 13)}$$

$$IIDR_{PM}\ (\frac{\mu g}{ml.min}) = 15.9 \times \exp(-0.045 \times ABZ\%) \qquad \text{(Eq. 14)}$$

The *IIDR* was almost independent in the 5% to 50% w/w drug concentration range for the SDs. The *IIDR* was enhanced for the SDs compared with the ABZ of pharmaceutical grade. The mechanism by which the drug is dissolved probably begins with the formation of a polymer-rich diffusion layer between the SD and the dissolution medium. After diffusion into this polymer-rich phase, the drug reaches the dissolution medium either as solvated molecules or as amorphous particles at a rate controlled by the carrier.

On the other hand, the *IIDR* for PMs was strongly influenced by the ABZ dissolution rate (drug controlled dissolution). The data were fitted adequately by an exponential equation (Eq. 14).

Finally, it is important to emphasize that *in vitro* solubility and dissolution studies represent an important link between the formulation design and its bioperformance. This is especially true for supersaturating formulations such as the SDs developed and evaluated in

this work. However, to stablish an *in vitro-in vivo* correlation (IVIVC), an *in vivo* parameter is needed, to relate it to the *in vitro* parameters. The replacement of *in vivo* testing with *in vitro* approaches presupposes well-based understanding of the scaling factors associating the *in vitro* with the *in vivo* measurements.

Conclusion

The results obtained revealed that the use of P 407 as carrier in ABZ SDs markedly improved its solubility and dissolution rate compared with pharmaceutical grade ABZ and a commercial formulation. The polymer maintained a desirable level of a supersaturation state in the dissolution medium by preventing solvent-mediated crystallization over the time period needed for the absorption process. However, SDs showed a better behavior than the PMs with the same P 407 proportion, observed in their higher initial dissolution rate and sampling time values, and lower dissolution times.

These approaches make SDs a very promising alternative strategy because the improvement of these properties could result in a faster absorption rate, and thus, in increased bioavailability of poorly water-soluble compounds as ABZ. However, further studies are required to advance in the development of these formulations considering the inherent thermodynamic instability associated to SDs, which could lead to relaxation, nucleation, and crystallization during storage. Undoubtedly, understanding the limits of the SDs and considering them when developing the drug delivery systems will be a key decision for the successful application of these materials. Moreover, further *in vivo* studies are necessary to evaluate the pharmacokinetic parameters of the SDs.

Future Perspective

It is expected that in the coming years there will be a considerable growth in the field of applications of solid dispersion to solve solubility-related challenges in pharmaceutical product development. This growth will be primarily driven by three factors: a) development and expansion of acceptable excipients, especially at the higher proportions needed for solid dispersions, b) application of newer technologies in the solid dispersions manufacture, and c) enhanced understanding of systems based on solid dispersions using predictive analytical tools to evaluated their stability and dissolution.

Executive summary

Physico-chemical characterization of Albendazole/Poloxamer solid dispersions

- Four solid dispersions with different albendazole/Poloxamer proportion were prepared and characterized, showing no chemical interaction between the two components.
- Albendazole phase solubility increased linearly (from 0.23 to 0.91 mg/ml) along with the Poloxamer concentrations in the solution from 0% to 15% (w/v).
- Polymer at 95 %w/w caused an increase in ABZ saturation solubility of about 4-fold with respect to solubility in the absence thereof.

Biopharmaceutical characterization

- Dissolution profiles were adjusted correctly with a mathematical model developed and validated by our research group, which allowed calculating pharmaceutical relevant parameters.
- Initial dissolution rate was 3 to 20-fold higher for solid dispersions than physical mixtures, pharmaceutical grade albendazole and a commercial formulation.
- The time needed to reach an 80% of dissolved drug was lower than 2.2 min for all the solid dispersions, indicating a fast dissolution.

- All solid dispersions presented higher dissolution efficiency than the other preparations.
- Based on the independent statistical analysis methods, difference and similarity factors indicated no significant differences between solid dispersions dissolution profiles.
- Mean dissolution time was similar for all the solid dispersions (between 6.7 and 8.2 min).

Financial disclosure

Authors would like to thank for the financial support to Agencia Nacional de Promoción Científica y Tecnológica (ANPCyT) [grant number PICT 2012-2643] and Consejo de Investigación Universidad Nacional de Salta (CIUNSa) [grant numbers 2199, 2398, 2392].

References

References of particular significance have been highlighted as: *** of interest**

1. Amidon GL, Lennernäs H, Shah VP, Crison JR. A theoretical basis for a biopharmaceutic drug classification: the correlation of *in vitro* drug product dissolution and *in vivo* bioavailability. *Pharm. Res.* 12(3), 413-420 (1995).
2. Thompson DO. Cyclodextrins—enabling excipients: their present and future use in pharmaceuticals. *Crit. Rev. Ther. Drug Carrier Syst.* 14(1), 1-104 (1997).
3. Pace SN, Pace GW, Parikh I, Mishra AK. Novel injectable formulations of insoluble drugs. *Pharm. Technol.* 23(3), 116-134 (1999).
4. Kawabata Y, Wada K, Nakatani M, Yamada S, Onoue S. Formulation design for poorly water-soluble drugs based on biopharmaceutics classification system: basic approaches and practical applications. *Int. J. Pharm.* 420(1), 1-10 (2011).
5. Vogt M, Kunath K, Dressman JB. Dissolution improvement of four poorly water soluble drugs by cogrinding with commonly used excipients. *Eur. J. Pharm. Biopharm.* 68(2), 330-337 (2008).
6. Dayan A. Albendazole, mebendazole and praziquantel. Review of non-clinical toxicity and pharmacokinetics. *Acta Trop.* 86(2), 141-159 (2003).
7. Wisher D. Martindale: the complete drug reference. *J. Med. Libr. Assoc.* 100(1), 75-77 (2012).
8. Jung H, Medina L, Garcia L, Fuentes I, Moreno-Esparza R. Biopharmaceutics: Absorption studies of

albendazole and some physicochemical properties of the drug and its metabolite albendazole sulphoxide. *J. Pharm. Pharmacol.* 50(1), 43-48 (1998).

9. Kasim NA, Whitehouse M, Ramachandran C *et al*. Molecular properties of WHO essential drugs and provisional biopharmaceutical classification. *Mol. Pharm.* 1(1), 85-96 (2004).

10. Rockville, MD. United States Pharmacopeial Convention. *United States Pharmacopeia and National Formulary* (USP 30-NF 25). Electronic version (2007).

11. Torrado S, Torrado S, Torrado JJ, Cadórniga R. Preparation, dissolution and characterization of albendazole solid dispersions. *Int. J. Pharm.* 140(2), 247-250 (1996).

12. Castro SG, Bruni SS, Lanusse CE, Allemandi DA, Palma SD. Improved albendazole dissolution rate in pluronic 188 solid dispersions. *AAPS PharmSciTech* 11(4), 1518-1525 (2010). *** of interest**
It describes the preparation and characterization of albendazole solid dispersions using Poloxamer 188 as carrier. This reference is of interest since it presents similar solid dispersions, but prepared using as carrier another member of poloxamers family, reaching lower percentages of dissolved ABZ.

13. Martinez-Marcos L, Lamprou DA, Mcburney RT, Halbert GW. A novel hot-melt extrusion formulation of albendazole for increasing dissolution properties. *Int. J. Pharm.* 499(1-2), 175-185 (2016).

14. Kalaiselvan R, Mohanta G, Manna P, Manavalan R. Studies on mechanism of enhanced dissolution of albendazole solid dispersions with crystalline carriers. *Indian J. Pharm. Sci.* 68(5), 599-607 (2006).

15. Palomares-Alonso F, Jung-Cook H, Pérez-Villanueva J *et al*. Synthesis and *in vitro* cysticidal activity of new benzimidazole derivatives. *Eur. J. Med. Chem.* 44(4), 1794-1800 (2009).

16. García A, Leonardi D, Lamas MC. Promising applications in drug delivery systems of a novel β-cyclodextrin derivative obtained by green synthesis. *Bioorg. Med. Chem. Lett.* 26(2), 602-608 (2016).

17. Rivera JC, Yépez-Mulia L, Hernández-Campos A *et al*. Biopharmaceutic evaluation of novel anthelmintic (1H-benzimidazol-5(6)-yl)carboxamide derivatives. *Int. J. Pharm.* 343(1–2), 159-165 (2007).

18. Mavrova AT, Vuchev D, Anichina K, Vassilev N. Synthesis, antitrichinnellosis and antiprotozoal activity of some novel thieno [2, 3-d] pyrimidin-4 (3H)-ones containing benzimidazole ring. *Eur. J. Med. Chem.* 45(12), 5856-5861 (2010).

19. Priotti J, Codina AV, Leonardi D, Vasconi MD, Hinrichsen LI, Lamas MC. Albendazole microcrystal formulations based on chitosan and cellulose derivatives: physicochemical characterization and *in vitro* parasiticidal activity in Trichinella spiralis adult worms. *AAPS PharmSciTech* 18(4), 947-956 (2017).

20. Paredes AJ, Llabot JM, Sánchez Bruni S, Allemandi D, Palma SD. Self-dispersible nanocrystals of albendazole produced by high pressure homogenization and spray-drying. *Drug Dev. Ind. Pharm.* 42(10), 1564-1570 (2016).

21. Naseri M, Akbarzadeh A, Spotin A, Akbari NaR, Mahami-Oskouei M, Ahmadpour E. Scolicidal and apoptotic activities of albendazole sulfoxide and albendazole sulfoxide-loaded PLGA-PEG as a novel nanopolymeric particle against *Echinococcus granulosus* protoscoleces. *Parasitol. Res.* 115(12), 4595-4603 (2016).

22. Kang B-S, Choi J-S, Lee S-E *et al*. Enhancing the *in vitro* anticancer activity of albendazole incorporated into chitosan-coated PLGA nanoparticles. *Carbohydr. Polym.* 159 39-47 (2017).

23. Kudtarkar A, Shinde U, P Bharkad G, Singh K. Solid lipid nanoparticles of albendazole for treatment of *Toxocara canis* infection: *in-vivo* efficacy studies. *Nanosci. Nanotechnol.-Asia* 7(1), 80-91 (2017).

24. Jelowdar A, Rafiei A, Abbaspour MR, Rashidi I, Rahdar M. Efficacy of combined albendazol and praziquantel and their loaded solid lipid nanoparticles components in chemoprophylaxis of experimental hydatidosis. *Asian Pac. J. Trop. Biomed.* 7(6), 549-554 (2017).

25. Chiou WL, Riegelman S. Pharmaceutical applications of solid dispersion systems. *J. Pharm. Sci.* 60(9), 1281-1302 (1971).

26. Vasconcelos T, Costa P. Development of a rapid dissolving ibuprofen solid dispersion. *Pharm. Res.* 16, 676-681 (2007).

27. Vo CL-N, Park C, Lee B-J. Current trends and future perspectives of solid dispersions containing poorly water-soluble drugs. *Eur. J. Pharm. Biopharm.* 85(3), 799-813 (2013).

28. Sekiguchi K, Obi N. Studies on absorption of eutectic mixture. I. A comparison of the behavior of eutectic mixture of sulfathiazole and that of ordinary sulfathiazole in man. *Chem. Pharm. Bull.* 9(11), 866-872 (1961).

29. Levy G. Effect of particle size on dissolution and gastrointestinal absorption rates of pharmaceuticals. *Am. J. Pharm. Sci. Support. Public Health* 135, 78-92 (1963).

30. Kanig JL. Properties of fused mannitol in compressed tablets. *J. Pharm. Sci.* 53(2), 188-192 (1964).

31. Sekiguchi K, Obi N, Ueda Y. Studies on absorption of eutectic mixture. II. Absorption of fused conglomerates of chloramphenicol and urea in rabbits. *Chem. Pharm. Bull.* 12(2), 134-144 (1964).

32. Jana S, Ali SA, Nayak AK, Sen KK, Basu SK. Development of topical gel containing aceclofenac-crospovidone solid dispersion by "Quality by Design (QbD)" approach. *Chem. Eng. Res. Des.* 92(11), 2095-2105 (2014).

33. Ohara T, Kitamura S, Kitagawa T, Terada K. Dissolution mechanism of poorly water-soluble drug from extended release solid dispersion system with ethylcellulose and hydroxypropylmethylcellulose. *Int. J. Pharm.* 302(1-2), 95-102 (2005).

34. Desai J, Alexander K, Riga A. Characterization of polymeric dispersions of dimenhydrinate in ethyl cellulose for controlled release. *Int. J. Pharm.* 308(1), 115-123 (2006).

35. Martinez-Marcos L, Lamprou DA, Mcburney RT, Halbert GW. A novel hot-melt extrusion formulation of albendazole for increasing dissolution properties. *Int. J. Pharm.* 499(1–2), 175-185 (2016).

36. De los Santos CJJ, Pérez-Martínez JI, Gómez-Pantoja ME, Moyano JR. Enhancement of albendazole dissolution properties using solid dispersions with Gelucire 50/13 and PEG 15000. *J. Drug Deliv. Sci. Tech.* 42 261-272 (2017).

37. Rowe RC, Sheskey PJ, Quinn ME, Association AP, Press P. *Handbook of pharmaceutical excipients*. Pharmaceutical press London, 6, (2009).

38. Toribio L, Nozal M, Bernal J, Nieto E. Use of semipreparative supercritical fluid chromatography to

obtain small quantities of the albendazole sulfoxide enantiomers. *J. Chromatogr. A* 1011(1-2), 155-161 (2003).

39. Fernández-Colino A, Bermudez J, Arias F, Quinteros D, Gonzo E. Development of a mechanism and an accurate and simple mathematical model for the description of drug release: Application to a relevant example of acetazolamide-controlled release from a bio-inspired elastin-based hydrogel. *Mater. Sci. Eng. C* 61, 286-292 (2016). *** of interest**

It describes a new, simple and accurate mathematical model for fitting drug release data, developed by our research group. This is the first report of the Lumped model, which is used to fit the data from the dissolution profiles.

40. Romero AI, Villegas M, Cid AG, Parentis ML, Gonzo EE, Bermúdez JM. Validation of kinetic modeling of progesterone release from polymeric membranes. *Asian J. Pharm. Sci.* 13(1), 54-62 (2018). *** of interest**

In this paper, progesterone release from polymeric membranes was used to validate the Lumped model, previously proposed by our research group, and used in this work to calculate different parameters of pharmaceutical relevance.

41. Costa P, Lobo JMS. Modeling and comparison of dissolution profiles. *Eur. J. Pharm. Sci.* 13(2), 123-133 (2001). *** of interest**

This complete review describes different mathematical models available for fitting drug dissolution data and discusses the methods used to compared dissolution profiles. Many of the parameters calculated are defined in this publication, as well as the criterion to stablish similarities between different profiles.

42. Pranzo MB, Cruickshank D, Coruzzi M, Caira MR, Bettini R. Enantiotropically related albendazole polymorphs. *J. Pharm. Sci.* 99(9), 3731-3742 (2010).

43. Ei-Badry M, Hassan MA, Ibrahim MA, Elsaghir H. Performance of poloxamer 407 as hydrophilic carrier on the binary mixtures with nimesulide. *Farmacia* 61(6), 1137-1150 (2013).

44. Gunasekaran S, Uthra D. Vibrational spectra and qualitative analysis of albendazole and mebendazole. *Asian J. Chem.* 20(8), 6310 (2008).

45. Garala K, Joshi P, Shah M, Ramkishan A, Patel J. Formulation and evaluation of periodontal *in situ* gel. *Int. J. Pharm. Investig.* 3(1), 29-41 (2013).

46. Moyano J, Liro J, Pérez J, Arias M, Sánchez-Soto P. Thermal analysis of albendazole investigated by HSM, DSC and FTIR. *Resonance (NMR)* 4 5 (2014).

47. Kabanov AV, Batrakova EV, Alakhov VY. Pluronic® block copolymers as novel polymer therapeutics for drug and gene delivery. *Journal of controlled release* 82(2-3), 189-212 (2002).

48. Jones M-C, Leroux J-C. Polymeric micelles – a new generation of colloidal drug carriers. *Eur. J. Pharm. Biopharm.* 48(2), 101-111 (1999).

49. Sharma A, Jain CP, Tanwar YS. Preparation and characterization of solid dispersions of carvedilol with poloxamer 188. *J. Chil. Chem. Soc.* 58(1), 1553-1557 (2013).

50. Craig DQ. The mechanisms of drug release from solid dispersions in water-soluble polymers. *Int. J.*

Pharm. 231(2), 131-144 (2002).

51. Diaz DA, Colgan ST, Langer CS, Bandi NT, Likar MD, Van Alstine L. Dissolution similarity requirements: how similar or dissimilar are the global regulatory expectations? *AAPS J.* 18(1), 15-22 (2016).

52. Mathur V, Nagpal K, Singh SK, Mishra DN. Comparative release profile of sustained release matrix tablets of verapamil HCl. *Int. J. Pharm. Investig.* 3(1), 60 (2013).

53. Moore T, Croy S, Mallapragada S, Pandit N. Experimental investigation and mathematical modeling of Pluronic® F127 gel dissolution: drug release in stirred systems. *J. Control. Release* 67(2), 191-202 (2000).

Websites

101. Administración Nacional de Medicamentos, Alimentos y Tecnología Médica (Argentinta). http://www.anmat.gov.ar/boletin_anmat/diciembre_2012/Dispo_7340-12.pdf (Accessed 23 July 2018)1. Amidon GL, Lennernäs H, Shah VP, Crison JR. A theoretical basis for a biopharmaceutic drug classification: the correlation of in vitro drug product dissolution and in vivo bioavailability. *Pharmaceutical research* 12(3), 413-420 (1995).

2. Thompson DO. Cyclodextrins—enabling excipients: their present and future use in pharmaceuticals. *Critical Reviews™ in Therapeutic Drug Carrier Systems* 14(1), (1997).

3. Pace SN, Pace GW, Parikh I, Mishra AK. Novel injectable formulations of insoluble drugs. *Pharmaceutical technology* 23(3), 116-134 (1999).

4. Kawabata Y, Wada K, Nakatani M, Yamada S, Onoue S. Formulation design for poorly water-soluble drugs based on biopharmaceutics classification system: basic approaches and practical applications. *International journal of pharmaceutics* 420(1), 1-10 (2011).

5. Vogt M, Kunath K, Dressman JB. Dissolution improvement of four poorly water soluble drugs by cogrinding with commonly used excipients. *European journal of pharmaceutics and biopharmaceutics* 68(2), 330-337 (2008).

6. Dayan A. Albendazole, mebendazole and praziquantel. Review of non-clinical toxicity and pharmacokinetics. *Acta tropica* 86(2), 141-159 (2003).

7. Wisher D. Martindale: the complete drug reference. *Journal of the Medical Library Association* 100(1), 75-77 (2012).

8. Jung H, Medina L, Garcia L, Fuentes I, Moreno - Esparza R. Biopharmaceutics: Absorption studies of albendazole and some physicochemical properties of the drug and its metabolite albendazole sulphoxide. *Journal of pharmacy and pharmacology* 50(1), 43-48 (1998).

9. Kasim NA, Whitehouse M, Ramachandran C *et al*. Molecular properties of WHO essential drugs and provisional biopharmaceutical classification. *Molecular pharmaceutics* 1(1), 85-96 (2004).

10. Rockville M. The United States Pharmacopoeia 30, the National Formulary 25 US Pharmacopeial

Formatted: Font: 10 pt, Not Bold, Spanish (Argentina), Not Expanded by / Condensed by

Formatted: Spanish (Argentina)

Formatted: Spanish (Argentina)

Field Code Changed

Formatted: Font: 10 pt

Formatted: Font: 10 pt, Not Bold

Convention. *Electronic version* (2007).

11. Torrado S, Torrado S, Torrado JJ, Cadórniga R. Preparation, dissolution and characterization of albendazole solid dispersions. *International journal of pharmaceutics* 140(2), 247-250 (1996).
12. Castro SG, Bruni SS, Lanusse CE, Allemandi DA, Palma SD. Improved Albendazole Dissolution Rate in Pluronic 188 Solid Dispersions. *AAPS PharmSciTech* 11(4), 1518-1525 (2010).
13. Martinez-Marcos L, Lamprou DA, Meburney RT, Halbert GW. A novel hot melt extrusion formulation of albendazole for increasing dissolution properties. *International journal of pharmaceutics* 499(1-2), 175-185 (2016).
14. Kalaiselvan R, Mohanta G, Manna P, Manavalan R. Studies on mechanism of enhanced dissolution of albendazole solid dispersions with crystalline carriers. *Indian journal of pharmaceutical sciences* 68(5), (2006).
15. Palomares-Alonso F, Jung-Cook H, Pérez-Villanueva J *et al*. Synthesis and in vitro cysticidal activity of new benzimidazole derivatives. *European Journal of Medicinal Chemistry* 44(4), 1794-1800 (2009).
16. García A, Leonardi D, Lamas MC. Promising applications in drug delivery systems of a novel β-cyclodextrin derivative obtained by green synthesis. *Bioorganic & Medicinal Chemistry Letters* 26(2), 602-608 (2016).
17. Rivera JC, Yépez-Mulia L, Hernández-Campos A *et al*. Biopharmaceutic evaluation of novel anthelmintic (1H-benzimidazol-5(6)-yl)carboxamide derivatives. *International Journal of Pharmaceutics* 343(1–2), 159-165 (2007).
18. Mavrova AT, Vuchev D, Anichina K, Vassilev N. Synthesis, antitrichinnellosis and antiprotozoal activity of some novel thieno [2, 3-d] pyrimidin-4 (3H)-ones containing benzimidazole ring. *European journal of medicinal chemistry* 45(12), 5856-5861 (2010).
19. Priotti J, Codina AV, Leonardi D, Vasconi MD, Hinrichsen LI, Lamas MC. Albendazole microcrystal formulations based on chitosan and cellulose derivatives: physicochemical characterization and in vitro parasiticidal activity in Trichinella spiralis adult worms. *AAPS PharmSciTech* 18(4), 947-956 (2017).
20. Paredes AJ, Llabot JM, Sánchez Bruni S, Allemandi D, Palma SD. Self-dispersible nanocrystals of albendazole produced by high pressure homogenization and spray-drying. *Drug development and industrial pharmacy* 42(10), 1564-1570 (2016).
21. Naseri M, Akbarzadeh A, Spotin A, Akbari NaR, Mahami-Oskouei M, Ahmadpour E. Scolicidal and apoptotic activities of albendazole sulfoxide and albendazole sulfoxide-loaded PLGA-PEG as a novel nanopolymeric particle against Echinococcus granulosus protoscoleces. *Parasitology research* 115(12), 4595-4603 (2016).
22. Kang B-S, Choi J-S, Lee S-E *et al*. Enhancing the in vitro anticancer activity of albendazole incorporated into chitosan-coated PLGA nanoparticles. *Carbohydrate polymers* 159 39-47 (2017).
23. Kudtarkar A, Shinde U, P Bharkad G, Singh K. Solid Lipid Nanoparticles of Albendazole for Treatment of Toxocara Canis Infection: In-Vivo Efficacy Studies. *Nanoscience & Nanotechnology-Asia* 7(1), 80-91 (2017).

24. Jelowdar A, Rafiei A, Abbaspour MR, Rashidi I, Rahdar M. Efficacy of combined albendazol and praziquntel and their loaded solid lipid nanoparticles components in chemoprophylaxis of experimental hydatidosis. *Asian Pacific journal of tropical biomedicine* 7(6), 549-554 (2017).

25. Chiou WL, Riegelman S. Pharmaceutical applications of solid dispersion systems. *Journal of Pharmaceutical Sciences* 60(9), 1281-1302 (1971).

26. Vasconcelos T, Costa P. Development of a rapid dissolving ibuprofen solid dispersion. *Pharm Res* 16 676-681 (2007).

27. Vo CL-N, Park C, Lee B-J. Current trends and future perspectives of solid dispersions containing poorly water-soluble drugs. *European Journal of Pharmaceutics and Biopharmaceutics* 85(3), 799-813 (2013).

28. Sekiguchi K, Obi N. Studies on Absorption of Eutectic Mixture. I. A Comparison of the Behavior of Eutectic Mixture of Sulfathiazole and that of Ordinary Sulfathiazole in Man. *Chemical and Pharmaceutical Bulletin* 9(11), 866-872 (1961).

29. Levy G. Effect of particle size on dissolution and gastrointestinal absorption rates of pharmaceuticals. *American journal of pharmacy and the sciences supporting public health* 135 78-92 (1963).

30. Kanig JL. Properties of fused mannitol in compressed tablets. *Journal of pharmaceutical sciences* 53(2), 188-192 (1964).

31. Sekiguchi K, Obi N, Ueda Y. Studies on Absorption of Eutectic Mixture. II. Absorption of fused Conglomerates of Chloramphenicol and Urea in Rabbits. *Chemical and Pharmaceutical Bulletin* 12(2), 134-144 (1964).

32. Jana S, Ali SA, Nayak AK, Sen KK, Basu SK. Development of topical gel containing aceclofenac-crospovidone solid dispersion by "Quality by Design (QbD)" approach. *Chemical Engineering Research and Design* 92(11), 2095-2105 (2014).

33. Ohara T, Kitamura S, Kitagawa T, Terada K. Dissolution mechanism of poorly water-soluble drug from extended release solid dispersion system with ethylcellulose and hydroxypropylmethylcellulose. *International journal of pharmaceutics* 302(1-2), 95-102 (2005).

34. Desai J, Alexander K, Riga A. Characterization of polymeric dispersions of dimenhydrinate in ethyl cellulose for controlled release. *International journal of pharmaceutics* 308(1), 115-123 (2006).

35. Martinez-Marcos L, Lamprou DA, Mcburney RT, Halbert GW. A novel hot-melt extrusion formulation of albendazole for increasing dissolution properties. *International Journal of Pharmaceutics* 499(1–2), 175-185 (2016).

36. De Los Santos CJJ, Pérez-Martínez JI, Gómez-Pantoja ME, Moyano JR. Enhancement of albendazole dissolution properties using solid dispersions with Gelucire 50/13 and PEG 15000. *Journal of Drug Delivery Science and Technology* 42 261-272 (2017).

37. Rowe RC, Sheskey PJ, Quinn ME, Association AP, Press P. *Handbook of pharmaceutical excipients*. Pharmaceutical press London, 6, (2009).

38. Toribio L, Nozal M, Bernal J, Nieto E. Use of semipreparative supercritical fluid chromatography to obtain small quantities of the albendazole sulfoxide enantiomers. *Journal of Chromatography A*

1011(1-2), 155-161 (2003).

39. Fernández-Colino A, Bermudez J, Arias F, Quinteros D, Gonzo E. Development of a mechanism and an accurate and simple mathematical model for the description of drug release: Application to a relevant example of acetazolamide-controlled release from a bio-inspired elastin-based hydrogel. *Materials Science and Engineering: C* 61 286-292 (2016).

40. Romero AI, Villegas M, Cid AG, Parentis ML, Gonzo EE, Bermúdez JM. Validation of kinetic modeling of progesterone release from polymeric membranes. *Asian Journal of Pharmaceutical Sciences* (2017).

41. Costa P, Lobo JMS. Modeling and comparison of dissolution profiles. *European journal of pharmaceutical sciences* 13(2), 123-133 (2001).

42. Pranzo MB, Cruickshank D, Coruzzi M, Caira MR, Bettini R. Enantiotropically Related Albendazole Polymorphs. *Journal of Pharmaceutical Sciences* 99(9), 3731-3742 (2010).

43. El-Badry M, Hassan MA, Ibrahim MA, Elsaghir H. Performance of poloxamer 407 as hydrophilic carrier on the binary mixtures with nimesulide. *Farmacia* 61(6), 1137-1150 (2013).

44. Gunasekaran S, Uthra D. Vibrational spectra and qualitative analysis of albendazole and mebendazole. *Asian Journal of Chemistry* 20(8), 6310 (2008).

45. Garala K, Joshi P, Shah M, Ramkishan A, Patel J. Formulation and evaluation of periodontal in situ gel. *International journal of pharmaceutical investigation* 3(1), 29 (2013).

46. Moyano J, Liro J, Pérez J, Arias M, Sánchez-Soto P. Thermal analysis of albendazole investigated by HSM, DSC and FTIR. *resonance (NMR)* 4 5 (2014).

47. Kabanov AV, Batrakova EV, Alakhov VY. Pluronic® block copolymers as novel polymer therapeutics for drug and gene delivery. *Journal of controlled release* 82(2-3), 189-212 (2002).

48. Jones M-C, Leroux J-C. Polymeric micelles—a new generation of colloidal drug carriers. *European Journal of Pharmaceutics and Biopharmaceutics* 48(2), 101-111 (1999).

49. Sharma A, Jain CP, Tanwar YS. Preparation and characterization of solid dispersions of carvedilol with poloxamer 188. *Journal of the Chilean Chemical Society* 58(1), 1553-1557 (2013).

50. Craig DQ. The mechanisms of drug release from solid dispersions in water-soluble polymers. *International journal of pharmaceutics* 231(2), 131-144 (2002).

51. Diaz DA, Colgan ST, Langer CS, Bandi NT, Likar MD, Van Alstine L. Dissolution Similarity Requirements: How Similar or Dissimilar Are the Global Regulatory Expectations? *The AAPS Journal* 18(1), 15-22 (2016).

52. Mathur V, Nagpal K, Singh SK, Mishra DN. Comparative release profile of sustained release matrix tablets of verapamil HCl. *International journal of pharmaceutical investigation* 3(1), 60 (2013).

53. Moore T, Croy S, Mallapragada S, Pandit N. Experimental investigation and mathematical modeling of Pluronic® F127 gel dissolution: drug release in stirred systems. *Journal of controlled release* 67(2), 191-202 (2000).

Figure legends

Formatted: Left, Line spacing: single, Widow/Orphan control

Figure 1. XRD diffractograms of pharmaceutical grade ABZ, P 407, SD4 and PM4.

Figure 2. FTIR spectra of pharmaceutical grade ABZ, P 407, SD4 and PM4.

Figure 3. SEM images: a) pharmaceutical grade ABZ; b) P 407; c) SD3; d) SD4; e) PM3 and f) PM4.

Figure 4. DSC thermograms of pharmaceutical grade ABZ, P 407, SD4 and PM4.

Figure 5. ABZ saturation solubility in HCl 0.1 N in presence of increasing P 407 proportions.

Bar errors cannot be distinguished since they are smaller than the symbols used for experimental data average.

Figure 6. Dissolution profiles of ABZ in 0.1 N HCl.

Figure 7. ABZ initial intrinsic dissolution rate (*IIDR*).

Table Legends

Table 1. Parameters of the Lumped model, sampling times, dissolution time for 80% and dissolution efficiency for SDs, PMs, pharmaceutical grade ABZ and CF.

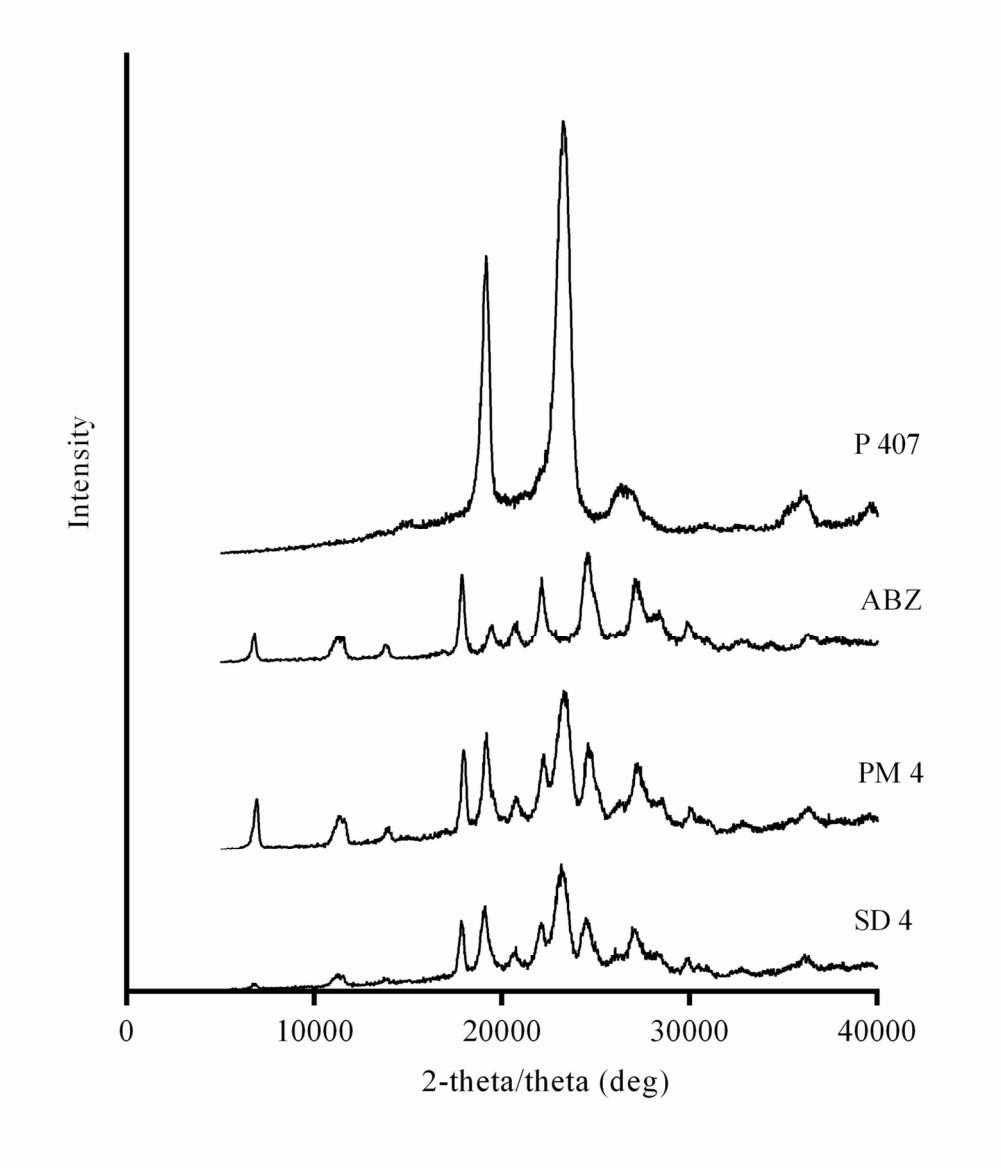

Figure 1. XRD diffractograms of pharmaceutical grade ABZ, P 407, SD4 and PM4.

125x147mm (300 x 300 DPI)

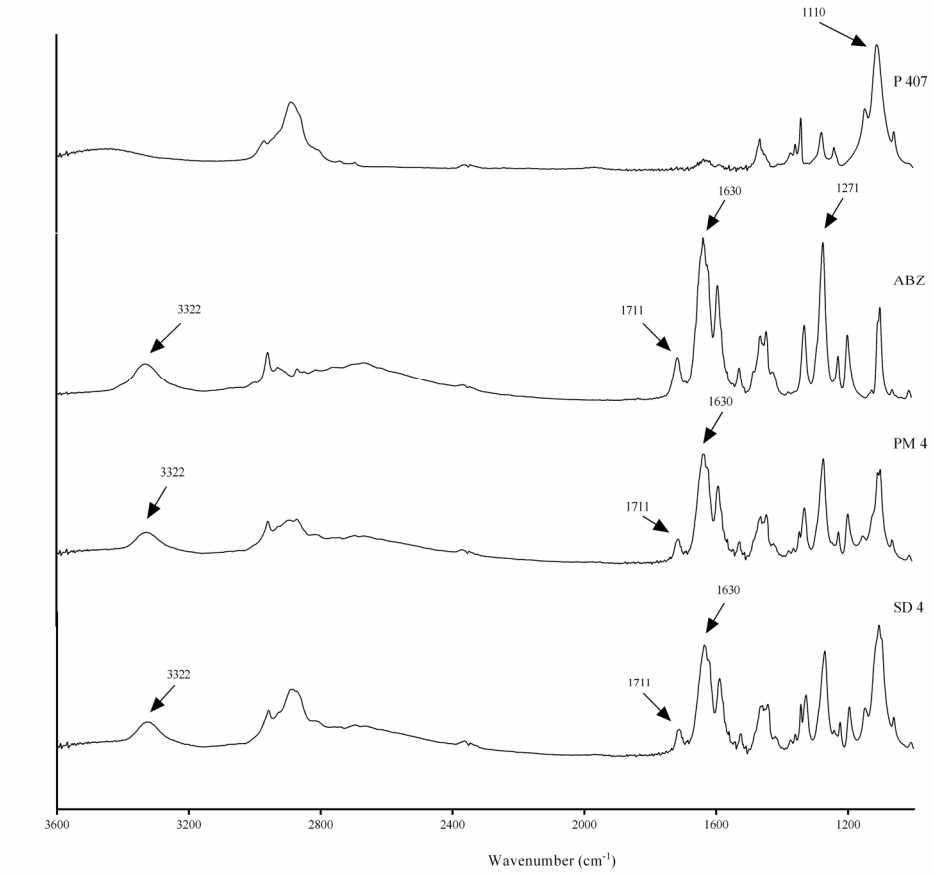

Figure 2. FTIR spectra of pharmaceutical grade ABZ, P 407, SD4 and PM4.

190x173mm (300 x 300 DPI)

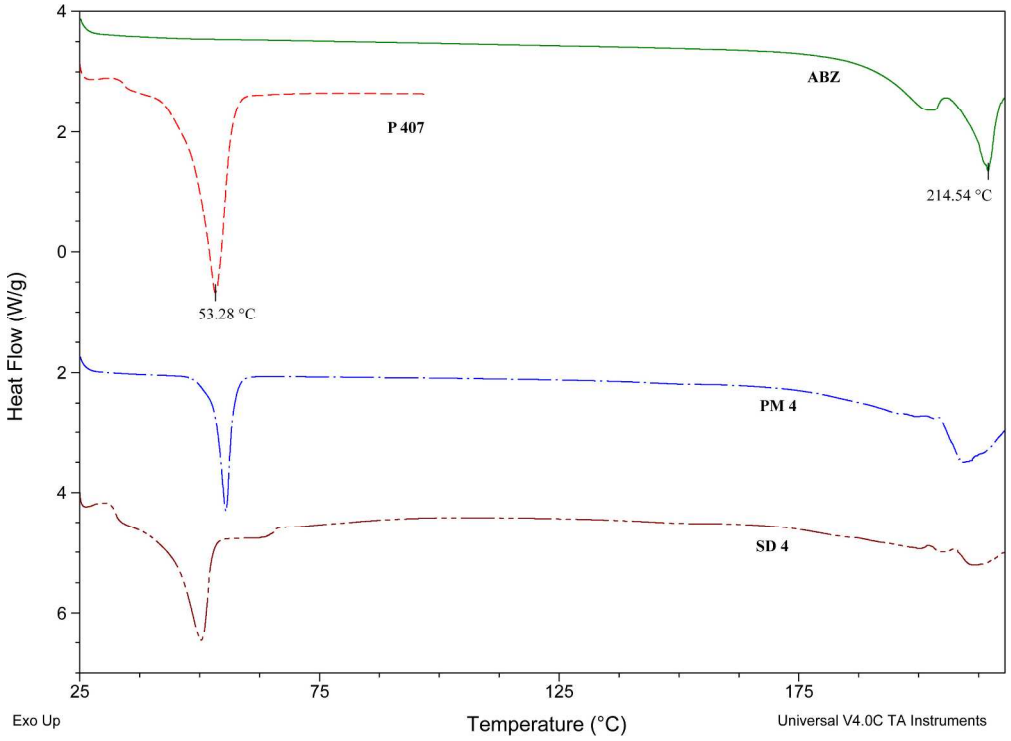

Figure 4. DSC thermograms of pharmaceutical grade ABZ, P 407, SD4 and PM4.

240x175mm (300 x 300 DPI)

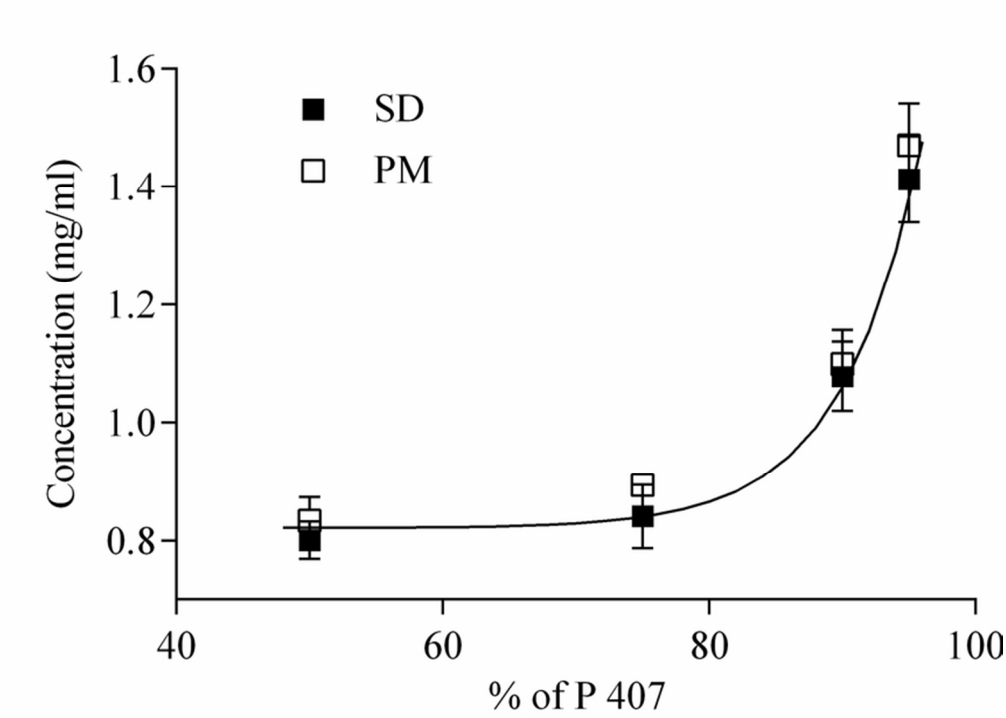

Figure 5. ABZ saturation solubility in HCl 0.1 N in presence of increasing P 407 proportions.
Bar errors cannot be distinguished since they are smaller than the symbols used for experimental data average.

72x55mm (300 x 300 DPI)

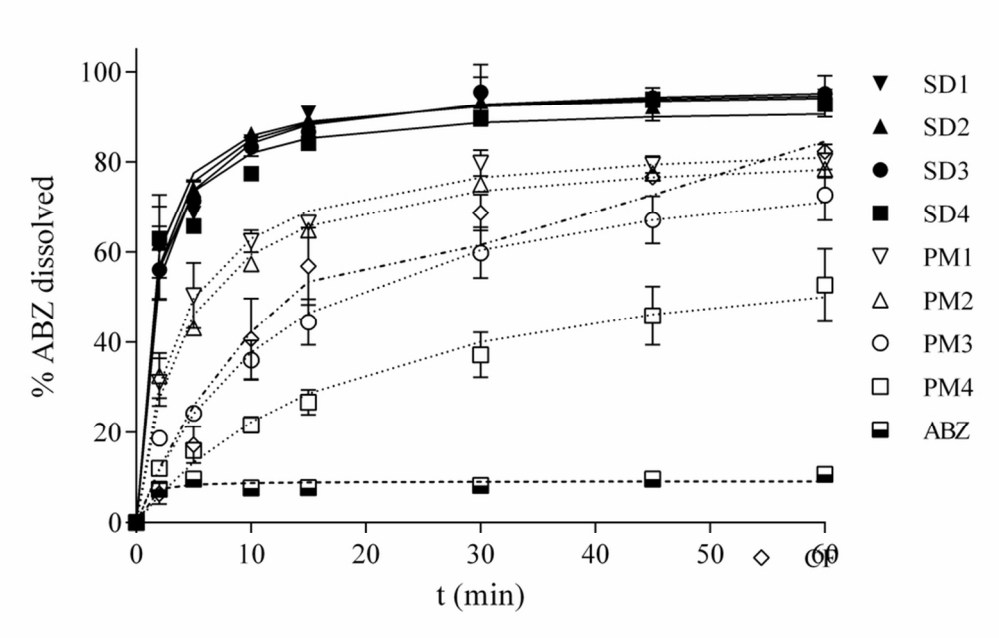

Figure 6. Dissolution profiles of ABZ in 0.1 N HCl.

86x55mm (300 x 300 DPI)

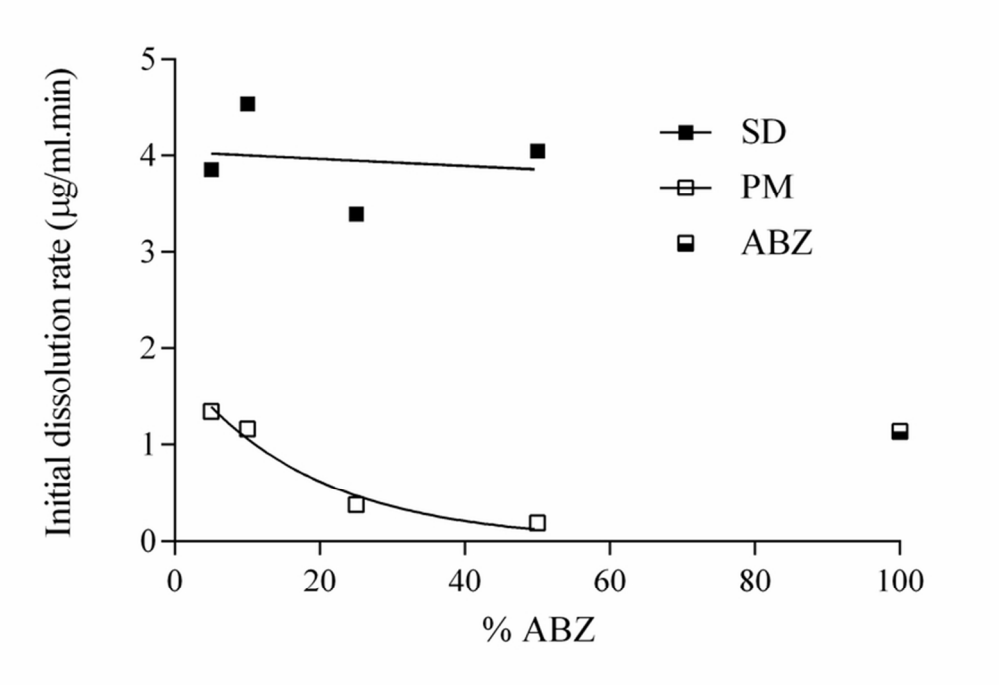

Figure 7. ABZ initial intrinsic dissolution rate (IIDR).

72x49mm (300 x 300 DPI)

Table 1 Parameters of the Lumped model, sampling times, dissolution time for 80% and dissolution efficiency for SDs, PMs, pharmaceutical grade ABZ and CF.

Sample	Parameters of the Lumped model			t_{tmin} (%)					$t_{80\%}$	DE
	a (% min^{-1})	b (min^{-1})	R^2	5	10	15	30	60	(min)	(%)
SD1	69.155	0.714	0.998	75.6	84.9	88.6	92.5	94.6	1.56	88.3
SD2	80.616	0.839	0.997	77.5	85.8	89.0	92.4	94.1	1.37	88.5
SD3	60.127	0.615	0.997	73.8	84.1	88.2	92.7	95.2	2.11	88.1
SD4	71.622	0.774	0.977	73.5	82.0	85.2	88.7	90.6	1.69	84.9
PM1	23.640	0.275	0.996	49.7	63.0	69.1	76.6	81.0	49.66	70.9
PM2	20.604	0.246	0.992	46.1	59.4	65.7	73.6	78.2	NR*	67.9
PM3	6.722	0.077	0.987	24.2	37.8	46.5	60.4	71.1	NR*	54.2
PM4	3.341	0.050	0.978	13.4	22.3	28.6	40.0	50.0	NR*	35.9
ABZ	19.640	2.140	0.904	8.4	8.8	8.9	9.0	9.1	NR*	8.8
CF	6.744	0.059	0.983	26.0	42.3	53.5	72.7	84.5	40.31	65.1

*NR: not reached

Close Window